Thermodynamic properties of magneto-anisotropic nanoparticles.

Malay Bandyopadhyay

Department of Theoretical Physics, Tata Institute of Fundamental Research, Colaba, Mumbai 400005, India.

E-mail: malay@theory.tifr.res.in

Abstract.

The purpose of this paper is to study the thermodynamic equilibrium properties of a collection of non-interacting three-dimensional (3D) magnetically anisotropic nanoparticles in the light of classical statistical physics. Pertaining to the angular dependence (α) of the magnetic field with the anisotropy axis, energy landscape plots are obtained which reveal a continuous transition from a double well to a single well for $\alpha = \frac{\pi}{2}$ and show asymmetric bistable shape for other values of α. The present analysis is related with the interpretation of equilibrium magnetization and static susceptibility of nanomagnetic system as a function of external magnetic field, B, and temperature, T. The magnetization and susceptibility confirms the non Langevin behaviour of magneto-anisotropic monodomain particles. The susceptibility analysis establishes the ferromagnetic, antiferromagnetic and paramagnetic like coupling for various α. This study reveals the essential role of magneto anisotropic energy in the interpretation of the magnetic behaviour of a collection of noninteracting single domain nanoparticles.

PACS numbers: 75.75.+a, 75.50.Tt, 75.40.Cx,75.20.-g

1. Introduction

Nanometer sized magnetic particles have provoked immense interest in both scientific as well as technological arena [1, 2, 3, 32, 5]. The development of intense fabrication techniques helps the preparation of nanoparticles with satisfactory structural and chemical properties. The study and analysis process gains acceleration due to the exaggerating growth of measurement facilities like magnetic force microscopy [6], micro-SQUIDS [7] and other magnetometry measurements [8, 9]. Such techniques have lead to the measurement of the magnetization process of single magnetic clusters in nanometer scales.

The magnetic moment of the nanoparticle consists of single domain structure of ferromagnetic spins with a large net spin, S ($\sim 10^3 - 10^4$) and hence it is named as supermoment [10, 11, 12]. This spin couples with a large number of environmental degrees of freedom of the host material. Dynamical disturbances of the surrounding environment leads to a rotational Brownian motion of the large spin surmounting the magnetic anisotropy potential barriers [13, 14]. In the high barrier limit, the magnetic response of the non-interacting single-domain particles follow the Neel relaxation process with the relaxation time τ characterized by the relation

$$\tau = \tau_0 \exp\big(\frac{\Delta E_a}{k_B T}\big), \tag{1}$$

where $\tau_0 \sim 10^{-10} - 10^{-13}$ sec. Here τ_0 is related to the intra-well motion and the height of the energy barrier due to anisotropy is $\Delta E_a = KV$ where K is the anisotropy constant, V is the particle volume, k_B is the Boltzmann constant and T denotes the absolute temperature. Depending on the relation of τ with the measurement time t_m, various interesting phenomena can be observed. For $\tau \ll t_m$, the magnetic moment exhibits the thermal equilibrium distribution of a paramagnet. For $\tau \gg t_m$, the magnetic moment stays very close to the energy minima as the reversal mechanism is blocked. For $\tau \sim t_m$, nonequilibrium phenomena i.e. magnetic relaxation is observed. In this work, all discussions are concentrated in the thermal equilibrium regime where $\tau \ll t_m$. In this context, the classical Stoner-Wohlfarth (SW) simplistic uniform rotation model of giant magnetic vector really provides insightful and realistic picture of magnetization reversal of single domain nanoparticle [15]. Here, we follow the same kind of arguments as proposed by Stoner and Wohlfarth [15].

The first study on the superparamagnetic behaviour of an aligned assembly of uniaxially anisotropic particles was made by F. G. West [16]. Further investigations regarding possible configurations encountered in experiment was made by Müller and Thurley[17]. Deviations from classical Langevin theory was demonstrated by several authors [18, 19, 20, 21, 22, 23]. Madsen *et al* have studied the effect of anisotropic energy on the interpretation of magnetization data for antiferromagnetic particles [24]. Vargas *et al* depicts a second order phase transition in non-interacting magneto-anisotropic nanoparticles when the external magnetic field is applied perpendicular to the anisotropy axis with the order parameter being the magnetization parallel to the field [25, 26]. Magneto-

caloric properties of noninteracting magneto-anisotropic nanoparticles have been studied in [30].

In this work, we investigate the effect of magneto-anisotropic energy on the equilibrium thermodynamic properties of fine particles. By thermal equilibrium behaviour, we meant that the measurement or observation time, t_m, is much larger than the characteristic relaxation time, τ, of the system i.e. we restrict our discussion in the regime $t_m \gg \tau$. On the other hand, below a certain critical size (for Fe, it is 150 nm.), it is not energetically favourable to form a domain wall, and the particle is said to be monodomain or fine particle system [11]. Having explained the terms "equilibrium properties" and "fine particles", we are now ready to describe briefly about our findings. Variations in the angle between the anisotropy axis and the external magnetic field, α, and between the former and the magnetic moment, θ, give deep insights into the thermodynamic equilibrium properties of magneto-anisotropic nanoparticles. We have extended the study of Vergas *et al* [25, 26] by choosing the magnetic moment and the anisotropy field vectors to be independent and arbitrary. On the other hand, Vergas *et al*, restricted their study for the particular case in which external field is perpendicular to the anisotropy axis. Also, we consider the particle size distribution of nanoparticles rather than the case of identical noninteracting particles as studied by Vergas *et al* [25, 26]. Thus the present study is much more realistic and close to the experimental realizations [27, 28, 29].

The variation of the magnetization and susceptibility with respect to external parameters like external field, B, and temperature, T, is extensively studied. The effect of anisotropy is evident from the magnetization versus reduced magnetic field, ξ, curve. The variation of inverse susceptibility with temperature for different angles, α, shows paramagnetic, ferromagnetic and antiferromagnetic like coupling which clearly exhibits the effect of mgneto-anisotropic energy on the static susceptibility of nanomagnetic system.

With the preceding background, the rest of the paper is organized as follows. In the next section, we discuss about the model system and other basic considerations about this model system. Section 3 deals with the model Hamiltonian and the relevent thermodynamic functions. In subsection 4.1, the energy landscape for the nanomagnetic system as a function of α is explored. The variation of equilibrium angle, θ, with dimensionless reduced magnetic field, h, for different α is demonstrated in the subsection 4.2. Section 5 deals with the variation of magnetization and susceptibility with respect to ξ and T. Finally, the paper is concluded in section 6.

2. Model and basic considerations

In this section, we discuss about our model and some basic considerations which one needs to study thermodynamic equilibrium properties of single domain particles. Kittle has shown that below a critical size, domain wall formation is energetically unfavourable [11]. This kind of particles are called single domain particles. In the absence of an ex-

ternal magnetic field, a bulk ferromagnet may have no net magnetization due to the cancellation from different domains. But, a single domain particle acts as a giant magnetic moment and the magnetic moment per particle depends on the particle volume and the number of atoms it has. Throughout this paper, we concentrate on the thermodynamic properties of a collection of such monodomain particles which are dispersed in solid matrix [31, 32]. Further, we restrict our study to mathematically tractable systems with axially symmetric magneto-anisotropy. But, it provides valuable insights into more complex situations. All our considerations are based on the Stoner-Wohlfarth model for single domain particles [15]. In this model, all spins within the particle are aligned due to exchange interaction and this is the dominating magnetostatic effect within the particle. The giant magnetic moment direction fluctuates, because the anisotropy energy is comparable to thermal energy. The direction of the moment is determined by the net anisotropy of the system and energy is minimized. This magnetization reversal process occurs by coherent rotation i.e. the atomic spins remain parallel to each other as they rotate to a new direction [13, 14]. Here, we are considering ideal monodomain particles in which other more complex interactions both within the particles and between the particles are neglected. Thus, our system has only magnetocrystaline energy and Zeeman energy due to the interaction with external field.

Now, we need to specify the validity of this model, especially in which temperature range it is valid. To specify this temperature range, we follow the arguments given by J. L. Garcìa Palacios [20]. It has already been mentioned that the thermal equilibrium behaviour of ideal monodomain particles with uniaxial anisotropy is observed when $t_m \gg \tau$. From equation (1), one can easily understand that thermal equilibrium behaviour exists when anisotropic potential barrier, ΔE_a, much larger than the thermal energy, k_BT. Besides, the "high-barrier" regime, equation (1) still holds down to $\Delta E_a/k_BT \geq 2$. It is known that τ_0 for magnetic nanoparticles is $\sim 10^{-10} - 10^{-12}$ sec. Thus, the thermal equilibrium range for a given measurement time, t_m, is given by $\ln\left(\frac{t_m}{\tau_0}\right) > \Delta E_a/k_BT \geq 0$. For magnetic measurements, $t_m \sim 1 - 100$ sec and the thermal equilibrium range is quite wide $25 > \Delta E_a/k_BT \geq 0$. So, the frequently encountered statement that the thermal equilibrium behaviour occurs when $\Delta E_a \geq k_BT$ is needlessly constrictive. For example, if $t_m = \tau_0 10^1 2$ sec (typical value for magnetic measurements), one finds that $\Delta E_a/k_BT \simeq 27.6$. For $\Delta E_a/k_BT = 25$, one can obtain $\tau = 0.08 t_m$. Thus, the system is in thermal equilibrium, but ΔE_a is still much larger than k_BT [20].

3. Hamiltonian and other relevent quantitites

We consider a collection of non-interacting single domain magnetic particles. In a single domain particle, nearly 10^5 magnetic moments are coherently locked together in a given direction thus yielding a supermoment. In this nanomagnetic system, every particle consists of a single magnetic domain with all its atomic moments are rotating coherently

and resulting in a constant absolute value of magnetization $m = m_s V$, where V is the volume of the particle and m_s is the saturation magnetization which is supposed to be independent of particle volume and temperature. In our system, the Hamiltonian consists of two parts, one representing the Zeeman energy and the other is the anisotropic energy (due to the crystalline structure of the particle). For the sake of simplicity, we consider a temperature independent uniaxial anisotropy. Denoting the external applied magnetic field as $\vec{B}$, the Hamiltonian is given by

$$\mathcal{H}(\vec{m}) = -\frac{KV}{m^2}\left(\vec{m}\cdot\hat{n}\right)^2 - \vec{m}\cdot\vec{B}, \tag{2}$$

where $\hat{n}$ is a unit vector along the anisotropy axis, $\vec{m}$ is the magnetic moment of the single domain particle and $\vec{B}$ is the direction of the external magnetic field as shown in Fig. 1 and K is the anisotropy constant. This model is valid only if the exchange

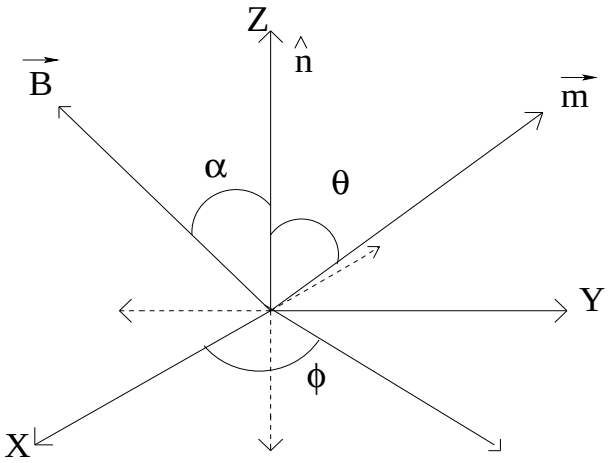

Figure 1. Coordinate system showing the unit vector along the anisotropy axis, $\hat{n}$, the external magnetic field vector, $\vec{B}$, and the magnetic moment vector, $\vec{m}$, along with the angles α, θ, and ϕ as referred in the text.

interaction strength of the system is much larger than K and B. Now denoting (θ, ϕ) and $(\alpha, 0)$ as the angular co-ordinates of $\vec{m}$ and $\vec{B}$ respectively and choosing $\hat{n}$ as the polar axis of the spherical polar co-ordinate system, one can write the total magnetic potential in the form as follows,

$$-\beta\mathcal{H} = \sigma\cos^2\theta + \xi_{\parallel}\cos\theta + \xi_{\perp}\sin\theta\cos\phi, \tag{3}$$

where $\sigma = \frac{KV}{k_B T}$, $\xi_{\parallel} = \xi\cos\alpha$, $\xi_{\perp} = \xi\sin\alpha$, $\xi = \frac{mB}{k_B T}$, $\beta = \frac{1}{k_B T}$, k_B is the Boltzman constant and T is the temperature of the system. One can rewrite Eq. (3) as follows

$$\mathcal{H}_{eff} = -\frac{\beta\mathcal{H}}{\sigma} = \cos^2\theta + 2h(\cos\alpha\cos\theta + \sin\alpha\sin\theta\cos\phi), \tag{4}$$

with $h = \frac{\xi}{2\sigma}$. Expressions for the magnetization curve where anisotropy is included have been discussed by [18, 19, 20, 21]. This calculation is based on the theory of Hanson *et al* [18] and Respaud [21]. For uniaxial anisotropic nanomagnetic system, the anisotropy energy depends only on the angle between the magnetization and the direction of easy

magnetization in the particle, θ. In thermal equilibrium, the magnetization in the direction of $\vec{m}$ is proportional to the Boltzmann factor for a fixed orientation of the easy axis :

$$f(\hat{m}) = z^{-1} \exp\Big[\sigma(\hat{m}\cdot\hat{n})^2 + \xi(\hat{m}\cdot\hat{h})\Big], \tag{5}$$

where $\hat{m}$, $\hat{h}$ are the unit vectors along the direction of magnetic moment and the external magnetic field and z is the partition function defined by

$$z = \int \exp\Big[(\hat{m}\cdot\hat{n})^2 + 2h(\hat{m}\cdot\hat{h})\Big]. \tag{6}$$

Thus, we have

$$\hat{m}\cdot\hat{h} = \cos\lambda = \sin\alpha\sin\theta\cos\phi + \cos\alpha\cos\theta \tag{7}$$

$$\hat{m}\cdot\hat{n} = \cos\theta. \tag{8}$$

Using the Boltzmann statistics, the expectation value of the reduced magnetization with a given orientation of the easy axis is given by

$$m(\alpha) = \frac{M}{m_s} = \langle\cos\lambda\rangle = \frac{\int_0^{2\pi} d\phi \int_0^{\pi} \cos\lambda e^{-\mathcal{H}_{eff}} \sin\theta d\theta}{\int_0^{2\pi} d\phi \int_0^{\pi} e^{-\mathcal{H}_{eff}} \sin\theta d\theta}. \tag{9}$$

None of the integrations in Eq. (9) is doable analytically. However, equation (9) can be simplified by using the modified Bessel functions and performing the analytic integration over ϕ. Thus, the magnetization of such a collection of non-interacting identical particles aligned with an angle α with respect to B is given by

$$m(\alpha) = \frac{N(\alpha)}{D(\alpha)}, \tag{10}$$

with

$$N(\alpha) = \int_0^{\pi} d\theta \sin\theta \exp(2h\cos\lambda + \cos^2\theta)[\sin\alpha\sin\theta I_1(2h\sin\alpha\sin\theta) + \cos\alpha\cos\theta I_0(2h\sin\alpha\sin\theta)], \tag{11}$$

$$D(\alpha) = \int_0^{\pi} d\theta \sin\theta \exp(2h\cos\lambda + \cos^2\theta) I_0(2h\sin\alpha\sin\theta), \tag{12}$$

where I_0 and I_1 are the modified Bessel function of order 0 and 1 respectively. Considering random distribution of anisotropy axes one can show

$$M_B(h) = \frac{1}{2}\int_0^{\pi} d\alpha \sin\alpha m(\alpha). \tag{13}$$

However, there will be a distribution of particle sizes in any real fine particle system. The existance of particle size distribution can be taken into account by taking average over the full particle size distribution. Thus, the magnetization of such a system with a distribution of particle sizes is consists of the sum of contributions from the superparamagnetic and the blocked particles. The weightage of these two is maintained by the size distribution function of the particles, $f(y)$. Now, the magnetization for this polydispersive system is given by

$$M_{Pol} = \int_0^{y_{sp}} M_{sp}(y,h) f(y) dy + \int_{y_{sp}}^{\infty} M_B(h) f(y) dy, \tag{14}$$

where y is the reduced volume $\frac{V}{V_0}$ with the mean volume V_0 and $y_{sp} = \frac{V_{sp}}{V_0}$. V_{sp} is the critical volume for superparamagnetism which is given by $V_{sp} = \frac{25k_BT}{K}$. $M_{sp}(y,h)$ and $M_B(h)$ are the reduced magnetization for the superparamagnetic and blocked particles respectively. It is known that $M_{sp}(h,y) = m_sL(2\sigma yh)$ where Langevin function $L(x) = \coth(x) - \frac{1}{x}$. Usually such anisotropic nanomagnetic system follows log-normal distribution of particle size i.e.

$$f(y) = \frac{1}{\sqrt{2\pi}\gamma y}\exp\Big[-\frac{(\ln y)^2}{2\gamma^2}\Big], \tag{15}$$

where γ is the dispersion of the corresponding distribution. For the numerical integration, we have used the following parameters : $\gamma = 0.8$, $V_0 = \exp(-\gamma^2/2)$, and average blocking temperature, $\langle T_B\rangle = 15.5K$, [33]. T is measured in units of $\langle T_B\rangle$, and h is measured in units of m_sB/K.

Numerical integration programme in FORTRAN are performed to calculate magnetization for the monodispersive and the polydispersive system by using equation (13) and (14) respectively. Static magnetic susceptibility of the polydispersive system is defined as

$$\chi_{pol} = \frac{\partial M_{pol}}{\partial B}. \tag{16}$$

Now, we have defined our system and other essential thermodynamic functions. In the next two sections, we analyze the thermodynamic behaviour of such magneto-anisotropic nanomagnetic system.

4. Energy barrier and equilibrium angle

In this section, we discuss about the behaviour of the magnetic potential energy as a function of the several parameters used in the Hamiltonian of the present nanomagnetic system. The variation of equilibrium angle, θ, between magnetic moment and easy axis of magnetization as a function of h is also studied in this section.

4.1. Energy barrier

One can rewrite equation (4) as follows

$$U(\theta,\phi) = \frac{\beta H(\theta,\phi)}{\sigma} = \sin^2\theta - 2h(\cos\alpha\cos\theta + \sin\alpha\sin\theta\cos\phi), \tag{17}$$

where $\beta = \frac{1}{k_BT}$. The stationary points for Equation (17) occurs for $\phi = 0$ and $\phi = \pi$. The stationary point for $\phi = \pi$ corresponds to a maximum, so it is of no physical interest. On the other hand, stationary point $\phi = 0$ corresponds to a maxima at θ_m and minima at θ_1 and θ_2. One can determine two equilibrium directions of the magnetization associated with polar angles θ_1 and θ_2 (lie in the x-z plane) from the following condition

$$\frac{\partial U}{\partial\theta} = 0, \frac{\partial^2 U}{\partial\theta^2} > 0, \tag{18}$$

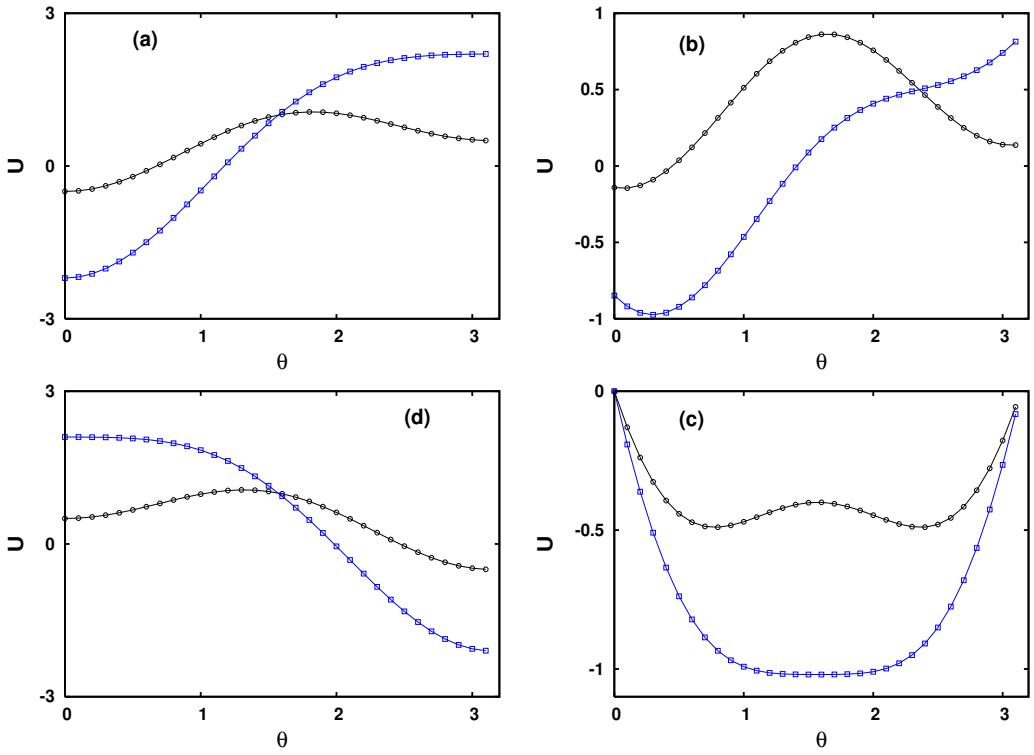

Figure 2. (color online) Energy is plotted against the angle θ for different cases with : (a) $\alpha = 0$ $\phi = 0$; $h = 0.25$ (black circle), and $h = 1.1$ (blue square) (b) $\alpha = \frac{\pi}{4}$ $\phi = 0$; $h = 0.1$ (black circle), and $h = 0.6$ (blue square) (c) $\alpha = \frac{\pi}{2}$ $\phi = 0$; $h = 0.7$ (black circle), $h = 1.01$ (blue square) (d) $\alpha = \pi$ $\phi = 0$; $h = 0.25$ (black circle), and $h = 1.1$ (blue circle).

and the saddle point is determined by

$$\frac{\partial U}{\partial \theta} = 0, \frac{\partial^2 U}{\partial \theta^2} < 0. \tag{19}$$

On the other hand, one can determine the critical value of the ratio of field to barrier height (h_c) at which the potential loses its bistable character by using the following condition

$$\frac{\partial U}{\partial \theta} = 0 = \frac{\partial^2 U}{\partial \theta^2}. \tag{20}$$

Using equation (20), one can easily show that [34]

$$h_c = \frac{1}{\left(\cos^{\frac{2}{3}}\alpha + \sin^{\frac{2}{3}}\alpha\right)^{\frac{3}{2}}}. \tag{21}$$

One can rewrite equation (21) as follows

$$(1 - h_c^2)^3 - \frac{27}{4} h_c^4 \sin^2 2\alpha = 0. \tag{22}$$

It can be shown that $|h_c|$ lies in the range $0.5 \leq |h_c| \leq 1$. $h_c = 1$ occurs for $\alpha = 0$ or $\alpha = \frac{\pi}{2}$. Whereas $h_c = \frac{1}{2}$ can be seen for $\alpha = \frac{\pi}{4}$. It is very unlikely that one can derive all the derivatives and hence the barrier heights (B_1 and B_2) for arbitrary

α. It is easy to derive barrier heights and to know the nature of the potential for some particular values of α. For $\alpha = 0$, $B_1 = \sigma(1+h)^2$ and $B_2 = \sigma(1-h)^2$. Thus the potential has the asymmetric bistable form as shown in Fig. 2(a). On the other hand, this asymmetric potential becomes symmetric and the barrier height becomes $B_1 = B_2 = \sigma(1-h)^2$ for $\alpha = \frac{\pi}{2}, \phi = 0$ (see figure 2(c)). Again for $\alpha = \frac{\pi}{4}$, the potential becomes asymmetric bistable below $h = 0.5$ (see figure 2(b)) and the barrier heights become [22] $B_1 = 2\sigma\sqrt{(1/2) - (h^2/2) - h\sqrt{(h^2/4) + (1/2)}}(\sqrt{(h^2/4) + (1/2)} - 3h/2)$ and $B_2 = B_1/2 + \sigma\sqrt{(1/2) - (h^2/2) + h\sqrt{(h^2/4) + (1/2)}}(\sqrt{(h^2/4) + (1/2)} + 3h/2)$. For $\alpha = \pi$, one can show that $B_1 = \sigma(1-h)^2$ and $B_2 = \sigma(1+h)^2$ and is just the opposite of the case for $\alpha = 0$ (see figure 2(d)). In general the potential retains its asymmetric bistable character for $0 < h < h_c$ and $\alpha \neq \frac{\pi}{2}$.
It is evident from fig. (2) that the potential energy of this nanomagnetic system has two minima separated by a maxima if and only if h is less than a ceratin critical value (h_c) which varies from 0.5 for $\alpha = \frac{\pi}{4}$ to 1.0 for $\alpha = 0, \frac{\pi}{2}$. So, the system consists of two potential barriers B_1 and B_2 which are in general unequal except for the case of $\alpha = \frac{\pi}{2}$. If $h > h_c$ the bistable character of the potential disappears and the system has only a single maxima or a single minima. At $h = h_c$, the second minima becomes a point of inflexion which is clearly seen in figure (2).

4.2. Equilibrium Angle

Here, we are considering a collection of non-interacting magnetic single-domain nanoparticles in the presence of an external magnetic field. The variation of the equilibrium angle between the anisotropy axis and the magnetic moment, θ, versus h for such a collection of noninteracting nanomagnetic system is shown in Fig. 3. Now, using the maxima and minima condition of $U(\theta, \phi)$ as defined by equation (18) and equation (19), one can obtain the equilibrium angle for the magnetization direction in the x-z plane for some specific values of α. Finally, the expression for the equilibrium angle θ for $\phi = 0$ under different orientations of α are as follows :
(i) for $\alpha = 0$ and $\phi = 0$:

$$\theta_m = \cos^{-1}(-h), \theta_{1,2} = 0, \pi \tag{23}$$

i.e $U(\theta, \phi)$ has minima at $\theta_{1,2} = 0, \pi$ and maxima at $\theta_m = \cos^{-1}(-h)$.
(ii) For $\alpha = \frac{\pi}{4}$ and $\phi = 0$,
the minima of the potential are at $\theta = \theta_1 = \frac{\pi}{4} - \sin^{-1}\Big(-\frac{h}{2} + \frac{\sqrt{h^2+2}}{2}\Big); 0 \leq \theta_1 \leq \frac{\pi}{12}$ and at $\theta = \theta_2 = \frac{5\pi}{4} - \sin^{-1}\Big(\frac{h}{2} + \frac{\sqrt{h^2+2}}{2}\Big); \frac{3\pi}{4} \leq \theta_2 \leq \pi$. On the other hand, the magnetic potential has maxima at $\theta = \theta_m = \frac{\pi}{4} + \sin^{-1}\Big(\frac{h}{2} + \frac{\sqrt{h^2+2}}{2}\Big); \frac{\pi}{2} \leq \theta_m \leq \frac{3\pi}{4}$ [34].
(iii) For $\alpha = \frac{\pi}{2}$ and $\phi = 0$,
$U(\theta, \phi)$ has minima at $\theta = \theta_1 = \sin^{-1}(h)$ and $\theta = \theta_2 = \pi - \sin^{-1}(h)$ and maxima at

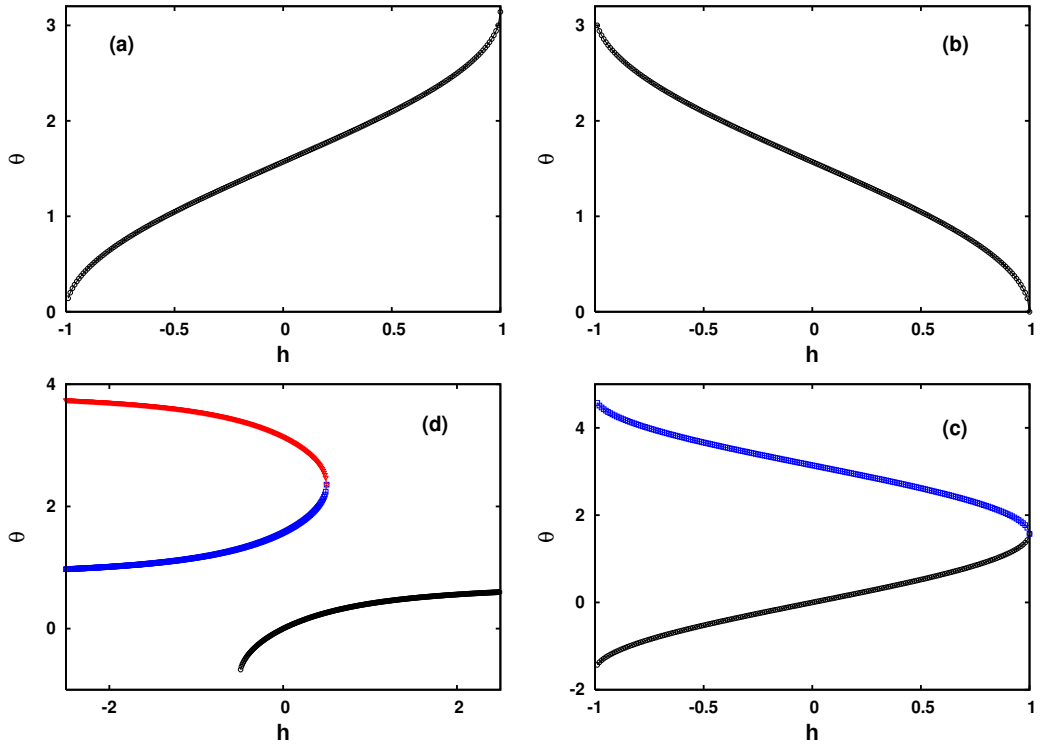

Figure 3. (color online) Plot of equilibrium angle, θ, versus h with $\phi = 0$ and (a) $\alpha = 0$ for θ_m (b) $\alpha = \pi$ for θ_m (c) $\alpha = \frac{\pi}{2}$; for θ_1 in black circle and θ_2 in blue square (d) $\alpha = \frac{\pi}{4}$; for θ_1 in black circle, θ_m in blue square and θ_2 in red triangle.

$\theta = \theta_m = \frac{\pi}{2}$.
(iv) and finally for $\alpha = \pi$ and $\phi = 0$ one can show that minima of the magnetic potential are at $\theta = \theta_{1,2} = 0, \pi$ and maxima at $\theta = \theta_m = \cos^{-1}(h)$.
In Fig. 3, we plot these solutions as a function of h. Figure 3(a) shows that θ_m for $\alpha = 0; \phi = 0$ increases from 0 to 3.0 as h is altered from -1 to $+1$. On the other hand, θ_m for $\alpha = \pi; \phi = 0$ decreases from 3.0 to 0 as h is varied from -1 to $+1$ (see fig. 3(b)). From figure 3(c), it is evident that as h is varied from -1 to $+1$, θ_1 increases from $-\frac{\pi}{2}$ to $\frac{\pi}{2}$ (black filled circle) and θ_2 decreases from $\frac{3\pi}{2}$ to $\frac{\pi}{2}$ (blue filled square). It is seen from fig. 3(d) that θ_1 (black filled circle) and θ_m (blue filled square) increases monotonically to a maximum value of $\frac{\pi}{12}$ and $\frac{3\pi}{4}$ respectively at $h = 0.5$; on the other hand, θ_2 decreases monotonically to a minimum value of $\frac{3\pi}{4}$ at $h = 0.5$ (red filled triangle).

5. Magnetization & Susceptibility

Magnetization and susceptibility are the most fundamental thermodynamical quantities of non-interacting magnetic nanoparticles with axially symmetric magnetic anisotropy. In this section, we analyze about the variation of these two fundamental quantities with temperature and externally applied magnetic field. The differences and similarities of

the magnetization and susceptibility between the ideal superparamagnetic system and a colletion of noninteracting anisotropic monodomain particles are presented here.

5.1. Magnetization

The magnetization along the direction of the external magnetic field for classical spins with axially symmetric magnetic anisotropy is defined by equation (13). We illustrate this magnetization as a function of ξ using equation (13) for a system of identical non-interacting monodomain particles for different values of σ in Fig. 4. One can easily

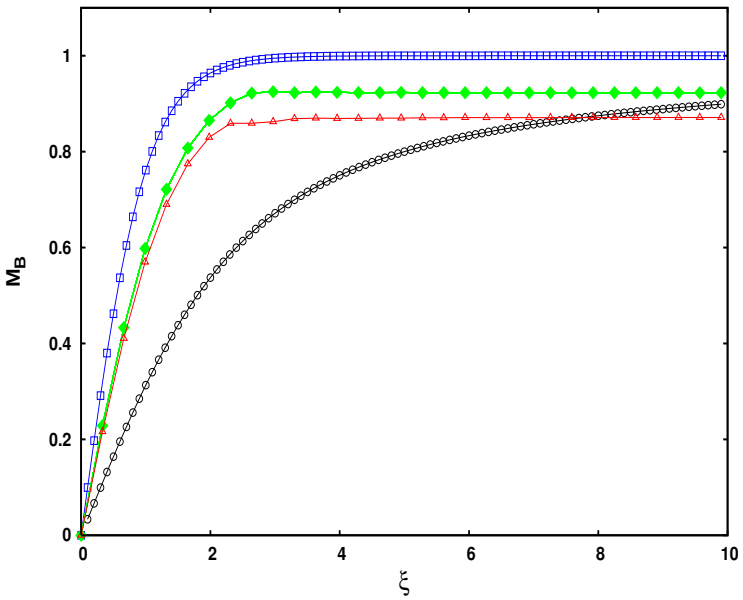

Figure 4. Reduced magnetization for the monodispersive system as a function of ξ, for various values of the anisotropy parameter, σ. The black circle and blue square represents Langevin ($\sigma = 0$) and Ising ($\sigma >> 1$) cases respectively. Green square and red upward triangle represents magnetization curves for $\sigma = 5.0$ and $\sigma = 2.0$ respectively.

observe that magnetization curves differ from the Langevin law in all the cases. As σ decreases, the difference vanishes and with the increase of σ, the magnetization curves become closer to the Ising case. In the limits of high and low field, ξ, magnetization, M_B, approaches the Langevin value. The largest influence of anisotropy can be observed in the intermediate field regime. This confirms the non-Langevin behaviour of a collection of noninteracting magneto-anisotropic single domain particles. In Fig. 5, we show the variation of magnetization with reduced temperature, $T_r = \frac{T}{\langle T_B \rangle}$, for two different values of h. Here $\langle T_B \rangle$ is the average blocking temperature of the system [35]. For convenience, we also plot the magnetization curves for the Ising and Langevin cases. It is clear that magnetization versus temperature curves for the anisotropic magnetic nanoparticle system show maximum near $T_r = 1.0$ unlike the Ising and Langevin cases.

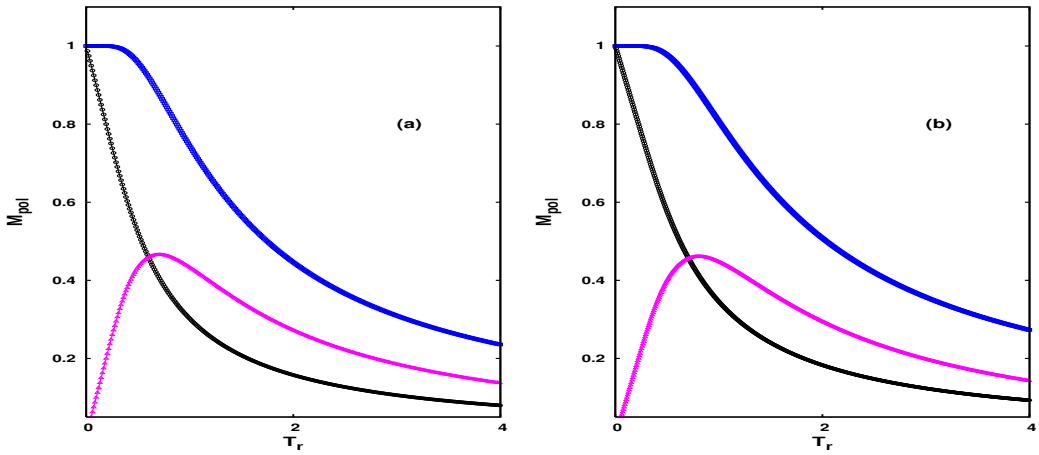

Figure 5. Reduced magnetization along the external field axis for a collection of noninteracting, monodomain and polydispersive nanoparticles as a function of reduced temperature. The black circle, blue square and pink upward triangle represents Langevin, Ising and magneto-anisotropic cases respectively: (a) h=0.2 and (b) h=0.5.

This maximum can be interpreted as follows. From equation (14), one can observe that M_{pol} has two parts, the superparamagnetic contribution and the blocked particle contribution. As the temperature increases the fraction of the superparamagnetic contribution increases till temperature reaches the blocking temperature. Now, above this blocking temperature at which maximum in magnetization is observed, the system usually becomes superparamagnetic and magnetization decreases rapidly with the increase of temperature due to the thermal agitation. Thus, in equilibrium and for $h < h_c$, one can observe maximum in magnetization for the polydisperse magneto-anisotropic nanoparticle system. One can observe that the maximum of the peak is exactly not at $T_r = 1.0$, but with the increase of field it shifts to lower relative temperature i.e. maximum are seen at $T_r = 0.89$ and at $T_r = 0.83$ for $h = 0.2$ and $h = 0.5$ respectively. Also one can notice that as the field increases, the peak becomes broader.

5.2. Susceptibility

In order to demonstrate the effect of magnetocrystalline anisotropy on the thermodynamical quantities, we demonstrate the behavior of susceptibility of the non-interacting nanoparticles in presence of an external magnetic field. We plot the susceptibility and inverse susceptibility curves with respect to temperature for different orientations in α between the anisotropy axis and external field in Fig. 6 and Fig. 7 respectively. Again, susceptibility shows a maximum at finite temperatures ($T_r = 0.89$ and $T_r = 0.83$) for $h = 0.2$ and $h = 0.5$ respectively. Also, as the field increases the peak of the susceptibility curves become more broader. In order to demonstrate the effect of magnetocrystalline anisotropy, we illustrate the behavior of inverse susceptibility of the noninteracting nanoparticles with reduced temperature in the presence of an external

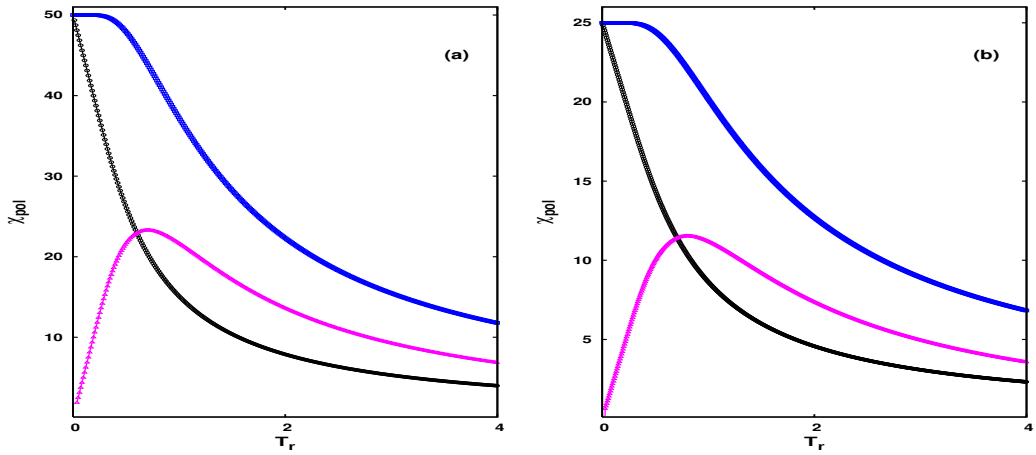

Figure 6. Static magnetic susceptibility along the external field axis for a collection of noninteracting, monodomain and polydispersive nanoparticles as a function of reduced temperature. The black circle, blue square and pink upward triangle represents Langevin, Ising and magneto-anisotropic cases respectively: (a) h=0.2 and (b) h=0.5.

magnetic field for different orientations of α between the anisotropy axis and external field in figure 7. For $\alpha = 0, \phi = 0$ (in black circle), one observes a susceptibility curve resembling a system with ferromagnetic like interaction and it follows Curie-Weiss law. The same kind of ferromagnetic like coupling is prevailed for $\alpha = \frac{\pi}{15}$ (in orange square) and for $\alpha = \frac{\pi}{10}$ (in pink upward triangle). This means the zero crossing at temperature axis occurs at positive values. When the angle between the anisotropy axis and magnetic field is $\alpha = \frac{\pi}{4}$ (in red downward triangle), the system resembles paramagnetic behavior and it follows simple Curie law. However, for $\alpha = \frac{\pi}{2}$ (in blue diamond) and for $\alpha = \frac{\pi}{3}$ (green filled square), a Curie-Weiss antiferromagnetic-like behavior is observed. By extrapolating one can observe the zero crossing in the temperature axis at negative values. Thus, the extrapolating transition temperature continuously changes from positive values to negative values. From this kind of observation, one can conclude that the anisotropy field acts as a ferromagnetic, antiferromagnetic or paramagnetic like coupling among the magnetic nanoparticles depending on the relative angle between the anisotropy axis and the external field. The net effect of the anisotropy field resembles a continupus transition from a ferromagnetic to an antiferromagnetic like coupling.

6. Conclusions

In conclusion, we have confirmed that a collection of noninteracting magneto-anisotropic particles cannot be described with the help of the classical Langevin theory, i.e., their thermodynamic equilibrium magnetization and static magnetic susceptibility cannot be described by the Langevin function and its derivative. This deviation is due to the presence of magneto-crystalline anisotropy. The effect of magnetocrystalline anisotropy

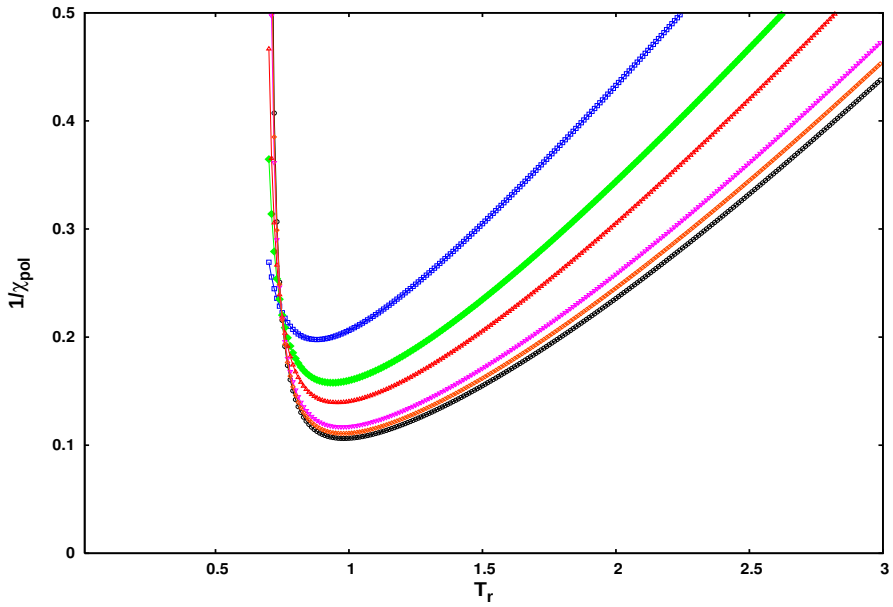

Figure 7. Inverse magnetic susceptibilities as a function of reduced temperature. Different curves represent different angles between anisotropy axis and external field (for details see text).

is explored through magnetization curves and susceptibility curves. The variation of inverse susceptibility with temperature shows paramagnetic, ferromagnetic and antiferromagnetic coupling behaviour for different orientations of α. We also present a mechanical analogy for a system in 3D as a frictionless particle moving on a sphere rotating about its vertical diameter. This study reveals the essential role of the magnetocrystalline anisotropy energy in interpreting equilibrium magnetization and susceptibility of a collection of non-interacting single domain nanomagnetic particles.

Appendix

In this appendix, we discuss about the mechanical isomorph of the nanomagnetic system. We consider a rigid sphere of radius R_s rotating along its vertical diameter at angular frequency ω with a frictionless particle of mass M free to move on the surface of the sphere. In the rotating co-ordinate frame (r, θ, ϕ) attached to the rigid sphere, in addition to the gravitational force on the mass $M\vec{g_a} = Mg_a \cos\theta \hat{e}_r - Mg_a \sin\theta \hat{e}_\theta$, a fictitious centrifugal force $\vec{f}$ is acting on the particle and is given by $\vec{f} = M\omega^2 r \sin^2\theta \hat{e}_r + M\omega^2 r \sin\theta\cos\theta \hat{e}_\theta$. An external field $\vec{F}$ is acting on the azimuthal plane such that $\vec{F} = F\sin\phi\hat{e}_\phi$. Now, the kinetic energy of the particle is given by

$$T = \frac{1}{2}M\Big(\dot{r}^2 + r^2\dot{\theta}^2 + r^2\sin^2\theta\dot{\phi}^2\Big). \tag{24}$$

The potential energy of the particle consists of three parts $U = U_{g_a} + U_c + U_e$, where U_{g_a} is coming from the gravitational force field part, U_c is the fictitious centrifugal part

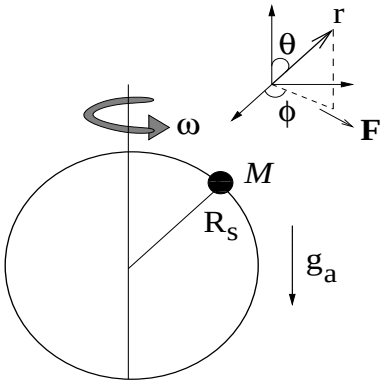

Figure 8. Mechanical rotating system analogous to nanomagnetic system

and U_e is the external field part. Now, one can easily find out the three parts of the effective potential energy as follows :

$$\begin{aligned} U_{g_a} &= -Mg_aR_s\cos\theta \\ U_c &= \frac{1}{2}M\omega^2R_s^2\cos^2\theta - \frac{1}{4}M\omega^2R_s^2 \\ U_e &= FR_s\sin\theta\cos\phi \end{aligned} \tag{25}$$

Thus the Lagrangian of the system becomes

$$\begin{aligned} \mathcal{L} = \frac{1}{2}M\left(\dot{r}^2 + r^2\dot{\theta}^2 + r^2\sin^2\theta\dot{\phi}^2\right) + Mg_aR_s\cos\theta \\ + \frac{1}{4}M\omega^2R_s^2 - \frac{1}{2}M\omega^2\cos^2\theta - FR_s\sin\theta\cos\phi. \end{aligned} \tag{26}$$

Now, the effective potential energy which includes the effect of gravity, rotation of the system and the external field force $\vec{F}$ is given by

$$u = \frac{U}{Mg_aR_s} = -\cos\theta - \frac{\omega^2R_s}{4g_a} + \frac{\omega^2R_s}{2g_a}\cos^2\theta + \frac{F}{Mg_a}\sin\theta\cos\phi. \tag{27}$$

Comparing equations (3) and (27) one can easily understand the analogy between the mechanical system and the magnetic nanoparticle system. The centripetal acceleration plays the role of the magnetic anisotropy, whereas the combined effect of external field $\vec{F}$ and the gravity field is equivalent to the external magnetic field.

[1] J. L. Dormann, D. Fiorani, and E. Tronc, Adv. Chem. Phys. *98*, 283 (1997).
[2] V. F. Puntes, K. M. Krishnan, and A. P. Alivisatos, Science *291*, 2115 (2001).
[3] J. Frankel and J. Dorfman, Nature (London) *126*, 274 (1930).
[4] S. Sun, C. B. Murray, D. Weller, L. Folks, and A. Moser, Science *287*, 1989 (2000).
[5] C. P. Bean and J. D. Livingstone, J. Appl. Phys. *30*, 120s (1959); I. S. Jacobs and C. P. Bean, *in magnetism* edited by G. T. Rado and H. Suhl (Academic, New York, 1963), Vol. III.
[6] M.Lederman, S.Schultz & M.Osaki, Phys. Rev. Lett. *73*, 1986 (1994).
[7] M. Jamet, W. Wernsdorfer, C. Thirion, D. Mailly, V. Dupuis, P. Mélinon and A. Pérez, Phys. Rev. Lett. *86*, 4676 (2001).
[8] A. D. Kent, T. M. Shaw, S. von Molnár, D. D. Awschalom, Science *262*, 1250 (1993).
[9] A. D. Kent, S. von Molnár, S. Gider, D. D. Awschalom, J. Appl. Phys. *76*, 6656 (1994).

[10] J. L. Dormann, D. Fiorani and E. Tronc, Adv. Chem. Phys. *98*, 283 (1997).
[11] C. Kittel, Phys. Rev. *70*, 965 (1946).
[12] A. Aharoni, Phys. Rev. A *135*, 447 (1964).
[13] L. Neel, Ann. Geophys. (C. N. R. S.) *5*, 99 (1949).
[14] W. F. Brown, Jr., Phys. Rev. *130*, 1677 (1963).
[15] E. C. Stoner and E. P. Wohlfarth, Philos. Trans. R. Soc., London, *240*, 599 (1948); IEEE Trans. Magn., *27*, 3475 (1991).
[16] F. G. West, J. Appl. Phys. *30*, 249s (1961).
[17] K. Müller, and F. Thurley, Int. J. Magn. *5*, 203 (1973).
[18] M. Hanson, C. Johansson, S. MØrup, J. Phys. Condens. Matt. *5*, 725 (1993).
[19] H. D. Williams, K. O'Grady, M. E. Hilo, R. W. Chantrell, J. Magn. Magn. Matt. *122*, 129 (1993).
[20] J. L. García-Palacios, in Advances in Chemical Physics, edited by I. Priogogine and Stuart A. Rice (John Wiley & Sons, 2000) Vol. *112*, 1 (2000).
[21] M. Respaud, J. Appl. Phys. *86*, 556 (1999).
[22] H. Pfeiffer, Phys. Stat. Sol. (a) *122*,377 (1990).
[23] H. Pfeiffer, Phys. Stat. Sol. (a) *120*,233 (1990).
[24] D. E. Madsen, S. MØrup, M. F. Hansen, J. Magn. Magn. Matt. *305*, 95 (2006).
[25] P.Vargas, D. Altbir, M. Knobel and D. Laroze, Euro. Phys. Lett. *58*, 603 (2002).
[26] P. Vargas and D. Laroze, J. Magn. Magn. Mat *272*, e1345 (2004).
[27] F. Wiekhorst, E. Shevchenko, H. Weller, and J. Kötzler, Phys. Rev. B *67*, 224416 (2003).
[28] S. Sun, C.B. Murray, D. Weller, L. Folks, and A. Moser, Science 287, 1989 (2000).
[29] E.V. Shevchenko, D.V. Talapin, A.L. Rogach, A. Kronowski, M. Haase, and H. Weller, J. Am. Chem. Soc. 124, 11 480 (2002).
[30] M. Bandyopadhyay and J. Bhattacharya, J. Phys.: Cond. Matt. *18*, 11309 (2006).
[31] S. Chakraverty, M. Bandyopadhyay, S. Chatterjee, S. Dattagupta, A. Frydman, S. Sengupta, and P. A. Sreeram, Phys. Rev. B *71*, 054401 (2005).
[32] Y. Sun, M. B. Salamon, K. Garnier, and R. S. Averback, Phys. Rev. Lett. 93, 139703 (2004).
[33] M. El-Hilo, K. O'Grady and R. W. Chantrell, J. Magn. Magn. Mater. *117*, 21 (1992).
[34] W. T. Coffey, D. S. F. Crothers, J. L. Dormann, L. J. Geoghegan, Yu. P. Kalmykov, J. T. Waldron, and A. W. Wickstead, Phys. Rev. B *52*, 15951 (1995).
[35] M. Bandyopadhyay and S. Dattagupta, Phys. Rev. B *74*, 214410 (2006).